

Received February 24, 2021, accepted March 8, 2021, date of publication March 10, 2021, date of current version March 19, 2021.

Digital Object Identifier 10.1109/ACCESS.2021.3065337

Comparative Study of Artificial Neural Network Based Channel Equalization Methods for mmWave Communications

DIEGO FERNANDO CARRERA^{id}, (Member, IEEE),
CESAR VARGAS-ROSALES^{id}, (Senior Member, IEEE),
NOE M. YUNGAICELA-NAULA^{id}, AND
LEYRE AZPILICUETA^{id}, (Senior Member, IEEE)

School of Engineering and Sciences, Tecnológico de Monterrey, Monterrey 64849, Mexico

Corresponding author: Diego Fernando Carrera (dfcarrera@ieee.org)

This work was supported by the Secretaría de Educación Pública (SEP)-Consejo Nacional de Ciencia y Tecnología (CONACyT) Research Project under Grant 255387, and in part by the School of Engineering and Sciences and the Telecommunications Research Focus Group with the Tecnológico de Monterrey.

ABSTRACT In this paper, we compare two artificial neural networks (ANNs) approaches designed to perform channel equalization for millimeter-wave (mmWave) signals operating in the 28 GHz frequency band. We used an in-house deterministic Three-Dimensional Ray-Launching (3D-RL) code to simulate the spatial structure of mmWave channels considering the material properties of the obstacles within the scenario at the frequency under analysis. We performed offline training of a multilayer perceptron (MLP) neural network with the simulated mmWave channels to equalize the received signal. We also performed online training of an extreme learning machine (ELM) neural network to directly get the equalized symbols at the receiver, given as input the received mmWave signal. The ANN solutions were tested in terms of the achievable spectral efficiency, bit error rate, and time to process. We compared the ANN techniques to the minimum mean square error and the zero-forcing equalizers, considering an orthogonal frequency-division multiplexing communication based on the 5G New Radio standard. We present numerical results on the performance of the proposed ANNs and show that the ELM strategy outperforms the MLP method, requiring significantly less processing time than the reviewed equalization methods.

INDEX TERMS 5G and beyond, channel equalization, ELM, multilayer perceptron, mmWave communications, OFDM.

I. INTRODUCTION

Although commercial millimeter-wave (mmWave) radios are already available, it could take two to five years for mmWave communications to become a mainstream technology used by end-users. This is due to the limited range of coverage of mmWave transmissions that demands a dense deployment of radio equipment, which implies that mobile service providers must invest more capital [1], [2]. Based on the fifth-generation (5G) New Radio (NR) standard, mmWave communications follow a cyclic prefix orthogonal frequency division multiplexing (CP-OFDM) scheme to transmit and receive the signals. At the receiver side, the signal processing

task is divided into several steps, such as channel estimation and interpolation, channel equalization, symbol demodulation, bit decoding, among others. To improve the operational efficiency of mmWave systems, multiple artificial intelligence (AI) strategies have been developed to achieve faster execution time at the signal processing level with highly parallel computing, through machine learning (ML) and deep learning (DL) methods [3].

Particularly, artificial neural networks (ANNs) have been applied in many tasks at the physical layer of wireless communications, and ANN strategies have been demonstrated to be successful in resolving these tasks in one step [4], [5]. With ANNs, the input-output behavior of a complex system is modeled by using model-free strategies, rather than relying on a mathematical expression as with traditional signal

The associate editor coordinating the review of this manuscript and approving it for publication was Donatella Darsena^{id}.

processing techniques. Nevertheless, it is important to recognize that many signal processing tasks, such as decision hard demodulation, have been solved optimally, and the solution approaches based on ANNs will not add further contributions in these applications [6]. On the other hand, ANNs are useful to learn specific tasks in the next-generation mobile networks, such as 5G and 6G, that are difficult to solve with traditional methods. Among these tasks, techniques of ML and DL are useful during beamforming establishment, channel estimation, signal detection, load balancing, and optimization of the available spectrum [7]. Using ML and DL algorithms present key advantages for complex analysis, and these techniques could save a considerable amount of computational power [2].

A. RELATED WORKS AND OUR CONTRIBUTIONS

Recent works have demonstrated that ANN approaches are suitable to solve different tasks in mobile communication systems. The work in [8] presents an ANN solution to perform channel estimation taking the estimated channel as an image input and performing an image re-scaling and restoration. This strategy is compared to the linear minimum mean squared error (MMSE) channel estimator. The results of this work are limited to the mean-squared error (MSE) and no equalization method was described. Authors of [9] present a Deep Neural Network (DNN) based channel estimation and tracking algorithm for vehicular mmWave communications. The simulation results showed that this approach estimates and tracks the mmWave channel efficiently and with minor training overhead. However, the analysis was limited to the MSE. The work in [4] presents a DNN design to perform channel equalization with OFDM systems. This approach addressed channel distortion and detected the transmitted symbols with performance comparable to the MMSE estimator. However, it is limited to a simple multipath channel model, which severely restricts the wireless characteristics of mmWave scenarios. The work presented in [10] explains that an estimation technique should be analyzed jointly with the channel equalization technique, since the MSE does not provide a wireless performance metric like the spectral efficiency (SE) or the bit error rate (BER). To the best of our knowledge, channel equalization depends directly on the accuracy of estimated channel and the technique used to perform this task. Therefore, it is of special interest to learn the equalization process with an ANN strategy in order to recover the received mmWave signal. However, this work is not centered on the estimation process since ANNs are capable of performing channel estimation and equalization in one single step.

Communication systems usually operate in dynamic and nonstationary environments in which conditions change over time. Therefore, ML/DL based solutions of these systems need to have mechanisms to detect and adapt to evolving data over time. Otherwise, their performance will degrade. This is where the extreme learning machine (ELM) algorithm comes in handy since this fully complex ANN has been recently

developed for recovering OFDM signals in wireless systems. The ELM algorithm can recover the OFDM signal with online training performed with reference signals (pilots) for single input single output (SISO) systems [11], [12]. However, a test of the performance of an ELM network has not been reported for mmWave frequencies where the path loss is high.

In this paper, a multilayer perceptron (MLP) neural network was designed to learn the specific task of channel equalization based on the minimum mean square error (MMSE) channel estimation and equalization. The MLP network takes as input the least squares (LS) estimation of the mmWave channel and provides as output the equalizer required to recover the received signal. We also designed an ELM neural network to directly equalize the received OFDM mmWave signal without performing offline training. Perfect channel state information (CSI) is not considered at the base station (BS), so the estimation of the CSI has been performed with the LS method to generate the dataset required to train the MLP network. Additionally, we consider realistic mmWave channels, based on an in-house deterministic Three-Dimensional Ray-Launching (3D-RL) algorithm, in which the full topological and material characteristics of the mobile scenario have been taken under consideration [13]. We run simulations of the mmWave CP-OFDM communication based on the Third Generation Partnership Project (3GPP), Release 15 specifications [14]. The contributions of this work are summarized as follows:

- We present a 3D-RL mmWave channel model in which full topological and material characteristics have been taken under consideration to generate the datasets for the ANNs.
- We trained an MLP neural network to learn the MMSE channel estimation and equalization process in one step, given as input of the neural network the LS estimation of the mmWave channel.
- We designed a real-time adaptive ELM network to directly equalize the received mmWave signals.
- We provide an analysis of the channel equalization performance of the MLP and ELM networks, in terms of the achievable SE, BER, and average time to process, and compared these techniques to the MMSE and zero forcing (ZF) channel equalizers.

II. BACKGROUND

A. SYSTEM MODEL

We consider a mmWave scenario, where a BS with a directive antenna communicates with single-antenna users in the 28 GHz frequency band. The SISO mmWave link employs N subcarriers to send data symbols, as is illustrated in Fig. 1 [15], [16]. Additionally, we consider a CP-OFDM communication system with 120 kHz of subcarrier spacing and time-division duplexing (TDD), according to the NR specifications described in the 3GPP Rel-15 standard [17].

We denote $\{\phi[k]\}_{k=0}^{N-1}$ as the k^{th} subcarrier pilot used by a user and transmitted with power ρ . To transmit the signal,

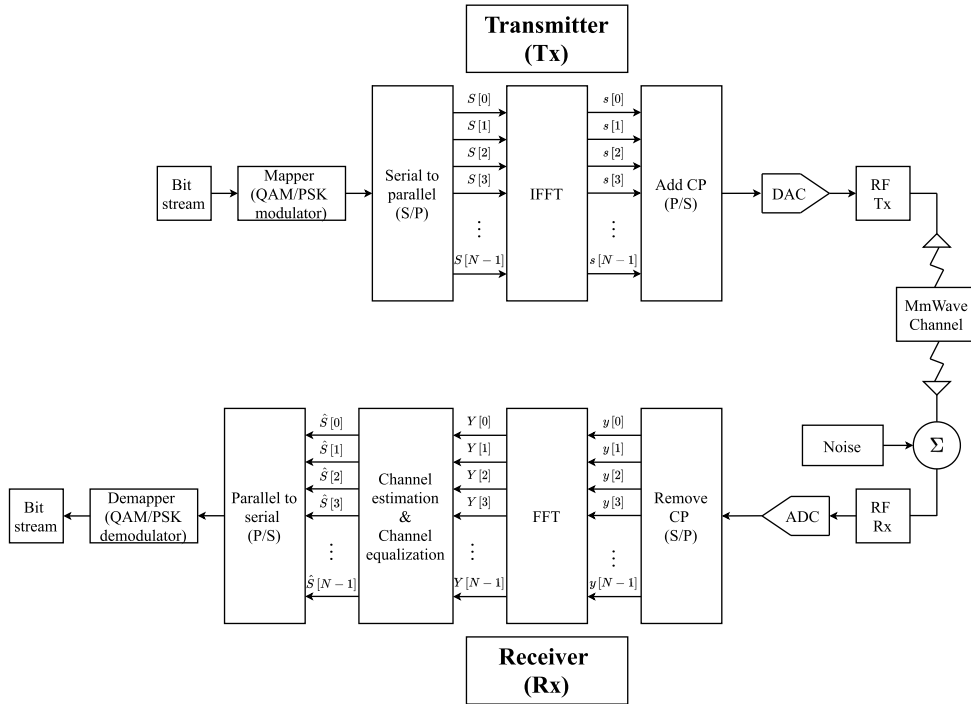


FIGURE 1. Simplified hardware block diagram of the CP-OFDM mmWave system.

it is necessary the use of a high power amplifier (HPA) which introduces nonlinear distortion. Considering the third-order statistic polynomial of the Volterra series, the amplified multicarrier pilot signal of the k^{th} subcarrier transmitted by a user is given by $\phi_k = X[k] + \eta X[k]|X[k]|^2$, where $\{X[k]\}_{k=0}^{N-1}$ is the pilot symbol mapped at the k^{th} subcarrier, and η is the HPA nonlinear distortion gain [17].

For coherent wireless communications systems, the BS needs to estimate the frequency-domain channel response at the k^{th} subcarrier, $\{H[k]\}_{k=0}^{N-1}$. The channel estimation process is performed with the received pilot signal at the k^{th} subcarrier, $\{Y_\phi[k]\}_{k=0}^{N-1}$, which can be written as

$$Y_\phi[k] = \sqrt{\rho}H[k]\phi[k] + Z[k] \quad (1)$$

where $\{Z[k]\}_{k=0}^{N-1}$ represents the Gaussian noise characterized as i.i.d $\mathcal{CN}(0, \sigma_Z^2)$ [18]. The LS estimate of the k^{th} subcarrier channel $\hat{H}[k]$ is given by

$$\hat{H}[k] = \frac{1}{\sqrt{\rho}}Y_\phi[k]\phi^*[k]. \quad (2)$$

For the LS estimation of the channels per subcarrier, it can be applied the MMSE estimation, which is a Bayesian approach to minimize the average MSE of the estimated channel $\hat{H}[k]$, given the received signal $Y[k]$, and is written as

$$\hat{H}_{mmse}[k] = \sigma_H^2(\sigma_H^2 + \sigma_Z^2)^{-1}\hat{H}[k] \quad (3)$$

where σ_H^2 represents the variance of the estimated subcarrier channels with LS [10], [19].

In (2), we assume the impact of interference is null due to the bandwidth available at mmWave frequencies. However, we consider that the impact of noise and nonlinear effects can significantly reduce the performance of the wireless system due to the high path loss characteristic of these signals. Similar to (1), the k^{th} subcarrier received signal $\{Y[k]\}_{k=0}^{N-1}$ at the BS during the uplink data transmission is given by

$$Y[k] = H[k]S[k] + Z[k] \quad (4)$$

where $\{S[k]\}_{k=0}^{N-1}$ represents the data symbols transmitted from the user.

To equalize the OFDM signal received in the uplink, it is necessary to calculate the frequency-domain equalizer per subcarrier, which is then multiplied with (4) to obtain

$$\hat{S}[k] = V[k]Y[k] = V[k]H[k]S[k] + V[k]Z[k], \quad (5)$$

where $\hat{S}[k]$ is the k^{th} equalized symbol, and $\{V[k]\}_{k=0}^{N-1}$ is the k^{th} subcarrier equalizer, which is based on the estimated channel $\{\hat{H}[k]\}_{k=0}^{N-1}$ through

$$V[k] = \begin{cases} (\hat{H}^*[k]\hat{H}[k])^{-1}\hat{H}^*[k], & \text{ZF} \\ (\hat{H}^*[k]\hat{H}[k] + \sigma_Z^2)^{-1}\hat{H}^*[k], & \text{MMSE}, \end{cases} \quad (6)$$

which corresponds to the ZF and MMSE channel equalizers, whereas $\{V^*[k]\}_{k=0}^{N-1}$ is used to pre-equalize the transmitted signal in the downlink [18]. Therefore, the important feature to learn with an ANN strategy is the channel equalizer, since it is used both in the uplink and downlink communication. In (6), we can use the LS channel $\hat{H}[k]$ estimation or the

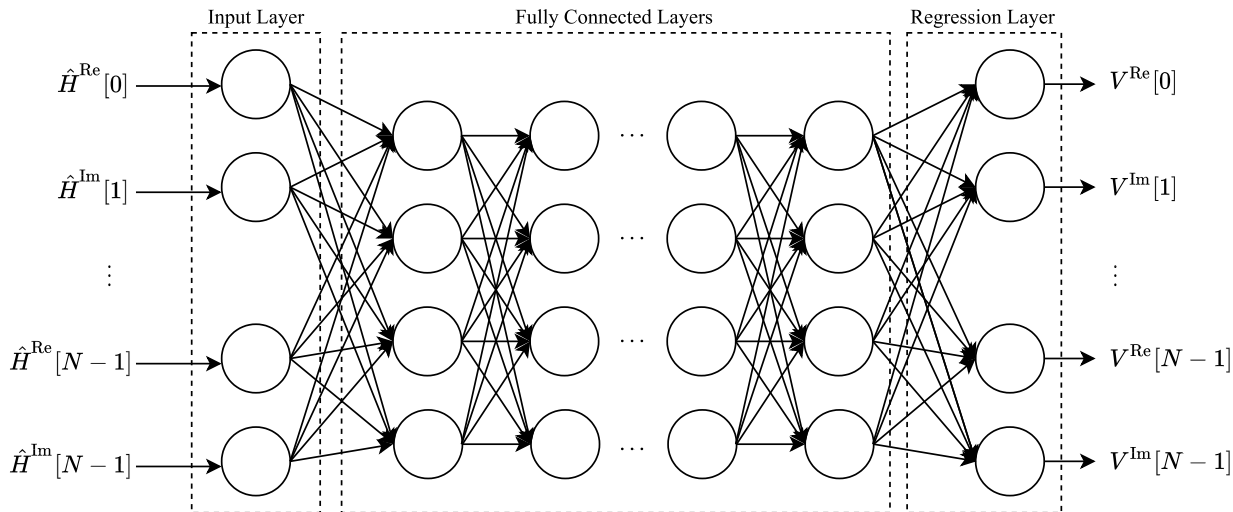


FIGURE 2. MLP neural network designed to perform channel equalization.

MMSE channel estimation $\hat{H}_{mmse}[k]$. The channel equalization presents a better performance with an accurate CSI. So, we used the MMSE channel estimation in this study in order to equalize the received signals and train the MLP neural network. However, more accurate channel estimators can be applied, which can potentially increase the performance of a given equalizer.

B. CHANNEL MODEL

The channel coefficients have been calculated by means of an in-house 3D-RL algorithm, optimized for mmWave frequency ranges [13], [20], [21]. The 3D-RL algorithm is based on geometrical optics (GO) and the geometrical theory of diffraction (GTD). The principle of the algorithm is that a set of rays are launched from the transmitter at a solid angle and the rays arriving at the receiver are considered the true path. Antenna radiation patterns can be introduced considering the elevation angle θ and the azimuth angle φ in the spherical coordinate system. The simulation scenario is discretized in an array of three-dimensional cuboids, according to the topology and dimensions of each scenario. The field components are then evaluated for the full simulation matrix. Electromagnetic phenomena such as reflection, refraction, and diffraction are considered, according to the material properties of all the obstacles within the environment at the operational system frequency. Based on [22], the channel frequency response from M paths can be calculated as follows

$$H[k] = \sum_{i=0}^{M-1} |h_i|^2 e^{-j2\pi f \tau_i}, \tag{7}$$

where $|h_i|^2$ is the power value of each multipath ray at the receiver, f is the carrier frequency and τ_i is the delay of each multipath. The in-house implemented 3D-RL algorithm has already been validated in the literature for different complex scenarios for mmWave frequency ranges. Some scenarios

which have been considered have been typical office scenarios [13], street urban canyon environments [20] or vehicular communications [21].

III. ARTIFICIAL NEURAL NETWORK STRATEGIES

A. MULTILAYER PERCEPTRON NETWORK-BASED EQUALIZER

In this section, we present an MLP neural network designed to perform MMSE channel estimation and equalization on the received OFDM signal in one single step. The MLP consists of multiple hidden layers that have greater learning and mapping capabilities than a single-layer neural network. The computation of the j^{th} neuron at each layer is given by

$$o_j = f\left(\sum_{i=1}^I (W_{ij} \times c_i + b_j)\right), \tag{8}$$

where b_j , o_j , c_i , W_{ij} and I are the bias, output data, input data, weights and the number of neurons respectively. $f(\cdot)$ is a non-linear function, called activation function, that is applied after a fully connected layer. The activation function allows us to generate nonlinear mappings.

The MLP neural network has shown high effectiveness in similar applications, such as channel estimation [23]. In this work, the MLP model was trained with the LS channel estimation performed with the pilot signals received in the uplink communication. The input of the network is the LS channel estimation, and the output corresponds to the k^{th} subcarrier equalizer $V[k]$, as is illustrated in Fig. 2.

The MLP method treats the input as an 1-D vector of real values. However, in a channel equalization scenario, the output is an 1-D vector of complex data. Therefore, the real and imaginary parts of this vector are input separately to the MLP neural network. That is, the training data is converted from a complex N-by-1 matrix into a real-valued 2N-by-1 matrix, where the real and imaginary parts are

concatenated subsequently, as shown in Fig. 2. The same strategy applies for the output of the MLP network, using the subcarrier equalizer signal. Formally, we show in Fig. 2 that the input of the MLP network corresponds to the real and imaginary parts of the LS estimated channel $\{\hat{H}^{\text{Re}}[k], \hat{H}^{\text{Im}}[k]\}_{k=0}^{N-1}$, and the output of the regression layer corresponds to real and imaginary parts of the equalizer $\{\hat{V}[k]^{\text{Re}}, \hat{V}[k]^{\text{Im}}\}_{k=0}^{N-1}$, for $k = 0, 1, 2, \dots, N - 1$.

B. ELM EQUALIZER

In [24], it is introduced an ELM-based receiver for massive multiple-input multiple-output (MIMO) systems, which can be applied for mmWave SISO communications as well. The advantage of this kind of receiver is that it can perform channel equalization online. Namely, it is not required to train the ELM network offline like with the MLP strategy. The ELM equalizer can be applied in the complex domain taking as input the received pilot signal vector $\mathbf{Y}_\phi = \{Y_\phi[0], Y_\phi[1], \dots, Y_\phi[N - 1]\} \in \mathbb{C}^N$ and as output the pilot vector $\phi = \{\phi[0], \phi[1], \dots, \phi[N - 1]\} \in \mathbb{C}^N$, a-priori known at the BS, as is illustrated in Fig. 3.

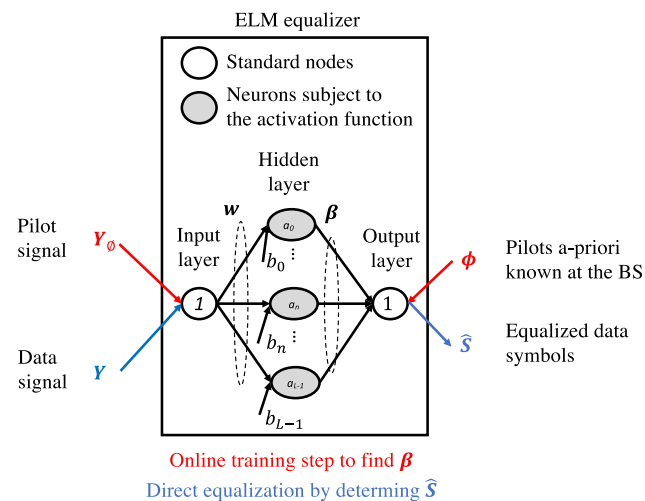


FIGURE 3. Complex domain ELM equalizer.

The ELM network, which consists of L hidden nodes, between the input and the output layers is written as $\phi = \mathbf{O}_\phi \beta$, where $\beta \in \mathbb{C}^L$ is the output weight vector, and $\mathbf{O}_\phi \in \mathbb{C}^{N \times L}$ represents the hidden layer output matrix when the pilot signal vector \mathbf{Y}_ϕ is used at the input of the ELM network. \mathbf{O}_ϕ is given by (9), as shown at the bottom of the page, where $a(\cdot)$ is the activation function of the hidden layer, $\mathbf{w} = [w_0, w_1 \dots, w_{L-1}] \in \mathbb{C}^L$ represents the weight vector between the single input neuron and the L hidden neurons,

and b_n denotes the bias of the n^{th} hidden node, for $n = 0, 1, \dots, L - 1$. Specifically, when $N > L$, the output weight vector is written as

$$\beta = (\mathbf{O}_\phi^h \mathbf{O}_\phi)^{-1} \mathbf{O}_\phi^h \phi. \tag{10}$$

After the ELM network is trained, the data signal vector $\mathbf{Y} = \{Y[0], Y[1], \dots, Y[N - 1]\} \in \mathbb{C}^N$ can be directly equalized, as $\hat{\mathbf{S}} = \mathbf{O} \beta$, where $\mathbf{O} \in \mathbb{C}^{N \times L}$ represents the hidden layer output matrix when \mathbf{Y} is used as the input of the network, which is given by (11), as shown at the bottom of the next page.

Finally, to equalize the received signal, it is necessary to use the output weight vector already learned from the training process and is written as

$$\hat{\mathbf{S}} = \mathbf{O} \beta, \tag{12}$$

where $\hat{\mathbf{S}} = \{\hat{S}[0], \hat{S}[1], \dots, \hat{S}[N - 1]\} \in \mathbb{C}^N$ denotes the equalized symbols at the output layer of the ELM network [12], [24].

IV. METHODS

In order to get the results, we performed extensive link-level simulations based on the 5G NR standard and the 3D-RL mmWave channel model introduced in Section II-B. We considered a CP-OFDM mmWave communication, and the reported results, namely SE, BER and time to process, were averaged over 8000 channel samples, which is equivalent to the number of 5G NR slots in one second of communication for 120 kHz of subcarrier spacing [17]. The simulation parameters are summarized in Table 1.

TABLE 1. 5G NR simulation parameters [17].

Parameter	Value
Carrier bandwidth	100 MHz
Carrier type	CP-OFDM (120kHz of subcarrier spacing)
Channel samples	8000
Channel estimation	LS and MMSE
Equalization method	ZF, MMSE, MLP, and ELM
HPA nonlinear gain η	$-0.03491 + i0.00567$
Occupied subcarriers	792 subcarriers per OFDM symbol
OFDM symbols per channel sample	14

The scenario illustrated in Fig. 4 was designed to simulate the frequency response of the mmWave channels. The outdoor scenario size is 70 x 175 meters, and the transmitter position was placed at $(x = 87.8 \text{ m}, y = 32.9 \text{ m}, z = 4 \text{ m})$ in a streetlight to analyze the link between the BS and a mobile device. For generating the mmWave channels and therefore simulating the dataset for the ANNs training, we use the

$$\mathbf{O}_\phi = \begin{bmatrix} a(w_0 Y_\phi[0] + b_0) & \cdots & a(w_{L-1} Y_\phi[0] + b_{L-1}) \\ \vdots & \ddots & \vdots \\ a(w_0 Y_\phi[N - 1] + b_0) & \cdots & a(w_{L-1} Y_\phi[N - 1] + b_{L-1}) \end{bmatrix} \tag{9}$$

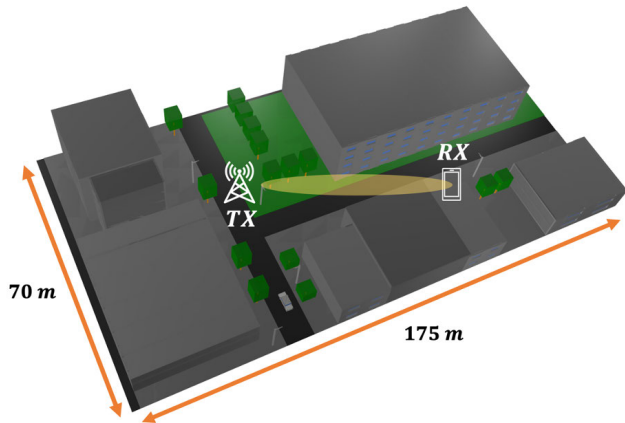


FIGURE 4. Schematic representation of the outdoor mmWave scenario.

3D-RL algorithm introduced in Section II-B for the 28GHz frequency band [13]. We performed the ray-launching simulations with a ray angular resolution of 1 degree in both azimuth and elevation, with the per ray upper bounds on six reflections and maximum ray path loss of 200 dB. The 3D-RL simulation parameters are summarized in Table 2.

TABLE 2. Scenario simulation parameters.

Parameter	Value
3D RL Resolution	1°
Antenna beam width	20°
Carrier frequency	28 GHz
Reflections	6
Scenario size (m)	70 x 175
Transmitter position	(87.8, 32.9, 4)
Transmitted power	10 dBm
Unitary volume analysis	1 m

A. DATASET GENERATION

We generated a dataset from simulations exclusively to perform offline training for the MLP neural network. First, we used 8000 channel samples to generate the estimated channel dataset, for which we used the LS method, and we also generated the equalizer dataset based on the MMSE channel estimation and equalization. Each LS channel estimation $\{H[k]\}_{k=0}^{N-1}$, and therefore each equalizer $\{V[k]\}_{k=0}^{N-1}$, consist of $N = 792$ subcarriers, which corresponds to the number of subcarriers available in a 100 MHz CP-OFDM communication with 120 kHz of subcarrier spacing.

For the total number of LS channels and MMSE equalizers, we used 80 % of the samples for the MLP training, 10 % for validation, and 10 % for testing.

B. MLP HYPERPARAMETERS TUNING

The hyper-parameters of the MLP model were selected using a random search approach. We first defined the maximum and minimum limits of the number of the fully connected layers, the number of neurons in each fully connected layer, and the training parameters, namely, the minibatch size and the number of epochs to train the model. In the case of the activation functions used in each layer, we defined two functions to be selected, namely, \tanh and $ReLU$. Then, we tested the hyper-parameters randomly, according to a uniform distribution, and selected the combination that produced the lower MSE on the validation set.

The best MLP neural network structure that resulted from the hyper-parameter selection was: An input layer with $2N$ neurons, corresponding to the real and imaginary components of the N subcarriers in the mmWave signal. It follows 10 fully connected layers with 120, 100, 120, 100, 120, 100, 120, 100, 120, and 100 neurons, respectively. After each fully connected layer, it follows a batch normalization layer that helps to speed up the training process of the ANN and reduce the sensitivity to network initialization. The activation function for each hidden layer is \tanh . Finally, we set the output regression layer with $2N$ neurons corresponding to the real and imaginary components of the N subcarriers. We used the stochastic gradient descent algorithm with momentum 0.9 and updated the network parameters with a learning rate of 0.001 and a mini-batch size of 600 samples. Moreover, we reduced the learning rate by a factor of 0.99 after each set of 10 epochs.

C. ELM PARAMETERS

The ELM network was designed to take as input the received pilot signal vector \mathbf{Y}_ϕ and as the output, the pilot vector ϕ , a priori known at the BS. This step is performed for the online training of the ELM network to find the output weigh vector β . After the training step, the input of the ELM network consists of the received data signal vector \mathbf{Y} to get as the output the equalized symbols vector $\hat{\mathbf{S}}$.

We used the \tanh activation function, which marginally outperforms other activation functions for ELM training [25]. The real and imaginary parts of the hidden layer parameters (\mathbf{w} and b_n) were arbitrarily assigned, following a uniform distribution in the interval $[-1, 1]$. Note that these parameters were kept fixed after the ELM network was trained [26]. Finally, we set 2 neurons for the hidden layer, since with fewer neurons, the ELM equalization performance degrades, and with more neurons, the results are the same.

$$\mathbf{O} = \begin{bmatrix} a(w_0 Y[0] + b_0) & \cdots & a(w_{L-1} Y[0] + b_{L-1}) \\ \vdots & \ddots & \vdots \\ a(w_0 Y[N-1] + b_0) & \cdots & a(w_{L-1} Y[N-1] + b_{L-1}) \end{bmatrix}. \quad (11)$$

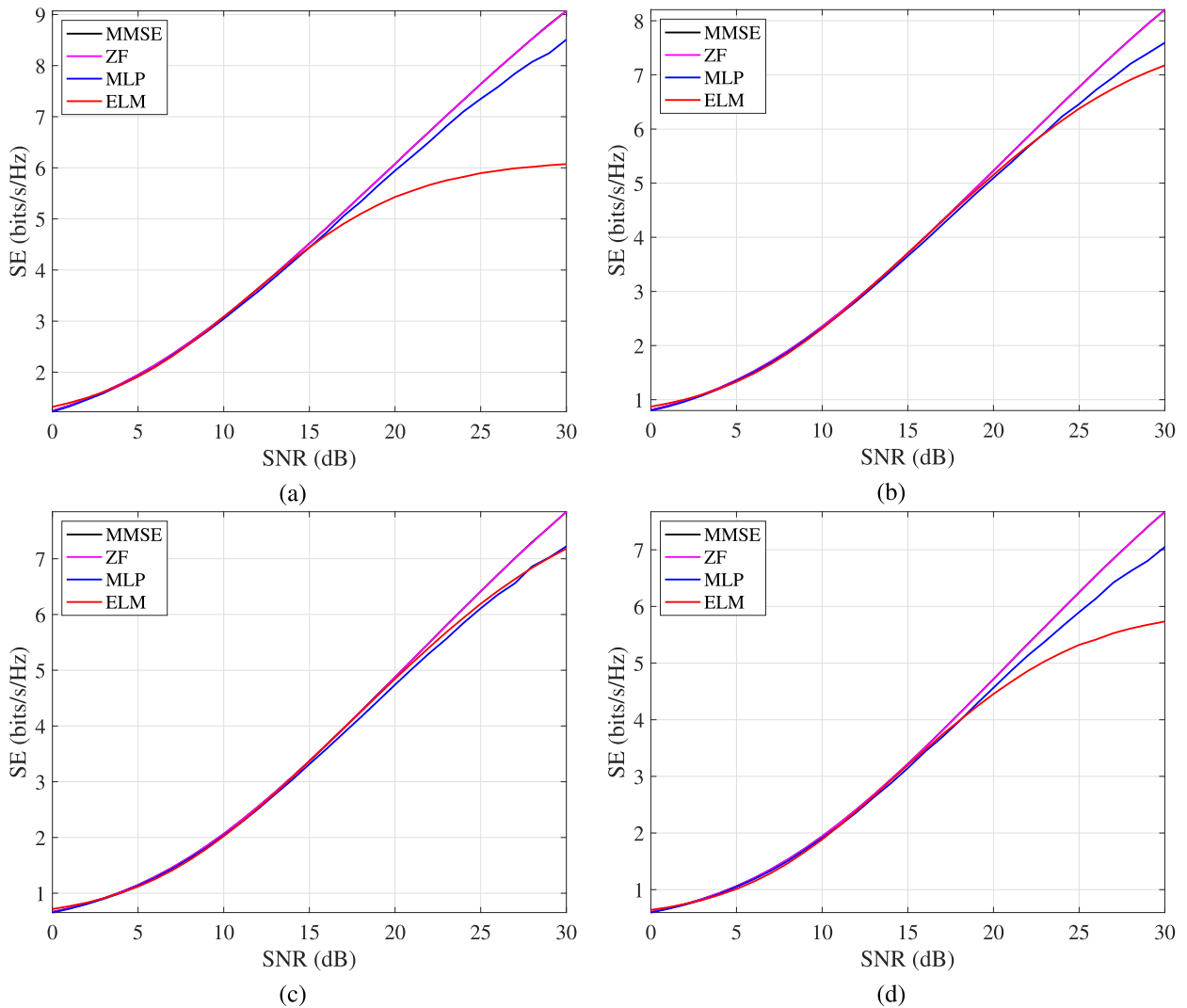


FIGURE 5. SE of the MMSE, ZF, MLP, and ELM equalization methods. (a) QPSK. (b) 16-QAM. (c) 64-QAM. (d) 256-QAM.

V. RESULTS AND DISCUSSION

With the simulation parameters of Table 1, we present the wireless performance results in terms of the achievable SE and BER for quadrature phase-shift keying (QPSK) modulation, 16-quadrature amplitude modulation (16-QAM), 64-QAM, and 256-QAM. These modulation schemes present different results, which depend on the signal-to-noise ratio (SNR) of the received signal. Fig. 5 shows the SE curves for MMSE and ZF channel equalization methods compared to the proposed MLP and ELM neural networks.

As is illustrated in Fig. 5, the SE of the MMSE and ZF channel equalization methods is the same for all the modulation schemes, and the MLP neural network achieves a SE closer to that achieved with the MMSE/ZF methods. The ELM strategy, on the other hand, presents the smallest SE for QPSK and 256-QAM modulations, however, for 16-QAM and 64-QAM, the SE of the ELM is similar to that achieved with the MLP strategy. However, only with the SE results

we cannot provide fair conclusions, so we present the BER results in Fig. 6 to determine the performance of the different techniques compared in this study.

Fig. 6 shows that the equalization methods perform almost equally for QPSK and 16-QAM. However, for 64-QAM and 256-QAM, the MLP and ELM strategies present higher BER than those achieved with the MMSE and ZF methods. Specifically, for 256-QAM, the ELM equalizer presents the highest BER of the compared methods. High order modulation schemes like 256-QAM require more SNR, which is a limiting factor for mmWave communications due to the high path loss that signals experience at those frequencies. On the other hand, the MLP strategy presents a smaller BER than that of the ELM method only for 256-QAM. However for QPSK, 16-QAM, and 64-QAM, the BER is higher with the MLP method. These results reveal that the ELM method is more accurate than the MLP strategy for the majority of the modulation schemes supported by the 5G NR standard.

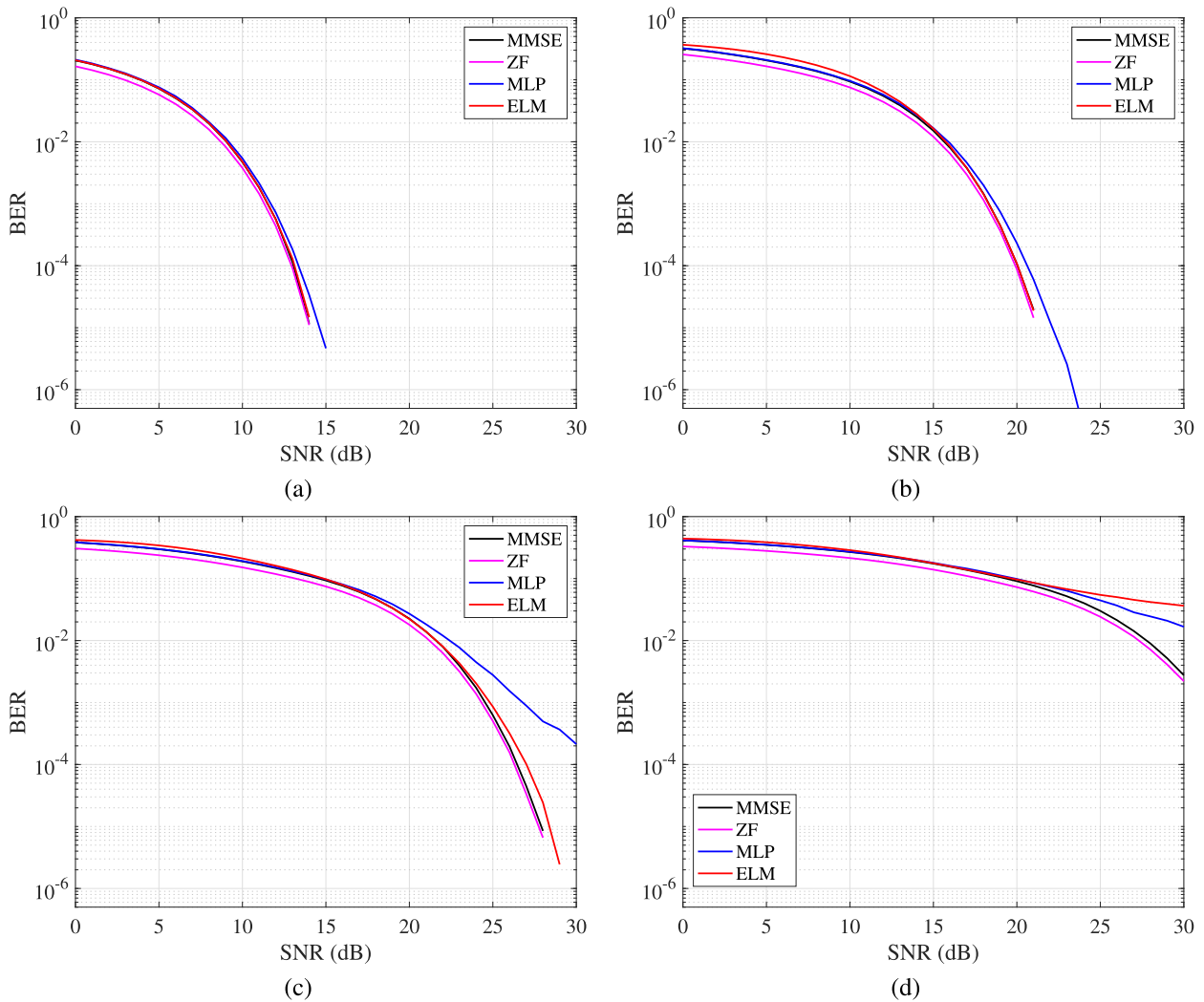


FIGURE 6. BER of the MMSE, ZF, MLP, and ELM equalization methods. (a) QPSK. (b) 16-QAM. (c) 64-QAM. (d) 256-QAM.

In Table 3 we present the time to equalize the received signal with the compared equalization methods. The processing time was averaged over 8000 channel realizations, and these results are useful to acknowledge the computational complexity of the compared methods.

TABLE 3. Time to process the channel equalization with MMSE, ZF, MLP and ELM.

Equalizer	Time to process (ms)
MMSE	9.6
ZF	9.5
MLP	116.8
ELM	3

For SISO systems, the ELM strategy requires at least 2 neurons in the hidden layer to perform the channel equalization task with low BER, which results in lower computational complexity than the other methods. However, the ELM strategy requires the pilot symbols to follow the same modulation scheme as the data symbols, which discard the standard

5G NR pilot structure. Compared to the ELM equalizer, the MLP strategy presents higher BER, but we can find the k^{th} subcarrier equalizer $V[k]$, which is useful to pre-equalize the mmWave signal for downlink transmission. However, this strategy requires a significant amount of time to perform channel equalization compared to the other studied methods, since it is required to process the signal only in the real domain.

If we consider an improved channel estimation technique in our study like recursive estimation [27], the results for the MMSE, ZF, and MLP strategies could be improved; however, for the ELM method there would be no change in the performance since this technique does not require to perform channel estimation, the ELM method performs channel equalization directly with the received signal. We considered MMSE channel estimation for the MMSE and ZF techniques, as well as to generate the dataset for training the MLP neural network since this estimation technique is well known and simple to process. In the Introduction Section,

we acknowledge that channel equalization depends directly on the accuracy of the estimated channel and the technique used to perform this task. So, with a better channel estimation technique, we can get better results, but only for the MMSE, ZF, and MLP equalizers.

Finally, we summarize the advantages and limitations of the proposed ANNs methods.

- **MLP advantages:** This strategy achieves good wireless performance (high) throughout the 5G NR supported modulation schemes. Only with an LS estimation input, we can directly perform channel equalization on the received signal. MLP training can be time-consuming and require high computational capabilities. However, once trained, the MLP model requires a limited number of floating point operations, which allows us to deploy this solution in real-time.
- **MLP limitations:** This strategy required a large dataset to achieve high levels of accuracy to learn the equalization process. That is, the learning processing needs elevated computational resources for the MLP training. However, given the latest CPU and GPU capabilities that have been customized for DL processes, this fact will not represent a relevant problem. Moreover, this model has a high component of “try and fail” and can have too many parameters that generate redundancy. Nevertheless, hyper-parameters optimization can help to minimize these issues. Finally, the MLP network must be trained offline, meaning that it is less adaptable than the ELM network. However, using parallel offline training will outperform this limitation.
- **ELM advantages:** The transmitted symbols can be recovered directly from the received signal, and the ELM training is performed with complex values. Furthermore, we highlight the real-time adaptation capabilities of this approach since the ELM performs online training on the received pilot signal, thus, the time to perform channel equalization is the shortest of the compared methods, which is the key advantage of this technique.
- **ELM limitations:** This ANN does not provide the equalizer value per subcarrier, which can be useful to pre-equalize the downlink signal. The achievable BER increases for 256-QAM, which requires more signal power than low-order modulation schemes like QPSK and 16-QAM.

VI. CONCLUSION

We experimented with two ANN strategies, namely, ELM and MLP neural networks, to perform channel equalization and achieve high wireless performance for SISO mmWave communications. The MLP neural network showed a performance comparable to that obtained with the MMSE and ZF channel equalizers for QPSK and 16-QAM; however, for high-order modulation schemes like 64 and 256-QAM, the BER increases. Given that the MLP network requires offline training, periodic MLP model retraining will be

needed to maintain its high performance in nonstationary systems. Nevertheless, with a large enough dataset, generated from a 3D-RL scenario, the offline training of the MLP network is more accurate, and the results can be compared without falling into optimistic parameters like perfect CSI. On the other hand, the ELM method can perform online channel equalization. Namely, this method does not require offline training like the MLP network and requires significantly less time to equalize the received signal compared to the other equalizers reviewed in this study, which turns this technique into a practical option to perform channel equalization at mmWave frequencies.

Finally, we highlight as a future research direction, the comparative analysis of ANNs for channel equalization in massive MIMO systems. With multiple antenna systems, the achievable BER is smaller, and therefore, the SE is higher due to the diversity gain of these systems. However, the complexity of signal processing also increases, so the computational complexity of the application of an ANN strategy is of special interest for future analysis.

REFERENCES

- [1] B. Gill and T. Bittman, “Hype cycle for edge computing, 2020,” Gartner, Stamford, CT, USA, Tech. Rep. G00450508, Jul. 2020.
- [2] O. Simeone, “A very brief introduction to machine learning with applications to communication systems,” *IEEE Trans. Cognit. Commun. Netw.*, vol. 4, no. 4, pp. 648–664, Dec. 2018.
- [3] H. Huang, S. Guo, G. Gui, Z. Yang, J. Zhang, H. Sari, and F. Adachi, “Deep learning for physical-layer 5G wireless techniques: Opportunities, challenges and solutions,” *IEEE Wireless Commun.*, vol. 27, no. 1, pp. 214–222, Feb. 2020.
- [4] H. Ye, G. Y. Li, and B.-H. Juang, “Power of deep learning for channel estimation and signal detection in OFDM systems,” *IEEE Wireless Commun. Lett.*, vol. 7, no. 1, pp. 114–117, Feb. 2018.
- [5] X. Gao, S. Jin, C.-K. Wen, and G. Y. Li, “ComNet: Combination of deep learning and expert knowledge in OFDM receivers,” *IEEE Commun. Lett.*, vol. 22, no. 12, pp. 2627–2630, Dec. 2018.
- [6] E. Bjornson and P. Giselsson, “Two applications of deep learning in the physical layer of communication systems [Lecture Notes],” *IEEE Signal Process. Mag.*, vol. 37, no. 5, pp. 134–140, Sep. 2020.
- [7] R. Chataut and R. Akl, “Massive MIMO systems for 5G and beyond networks—Overview, recent trends, challenges, and future research direction,” *Sensors*, vol. 20, no. 10, p. 2753, 2020.
- [8] M. Soltani, V. Pourahmadi, A. Mirzaei, and H. Sheikhzadeh, “Deep learning-based channel estimation,” *IEEE Commun. Lett.*, vol. 23, no. 4, pp. 652–655, Apr. 2019.
- [9] S. Moon, H. Kim, and I. Hwang, “Deep learning-based channel estimation and tracking for millimeter-wave vehicular communications,” *J. Commun. Netw.*, vol. 22, no. 3, pp. 177–184, Jun. 2020.
- [10] D. F. Carrera, C. Vargas-Rosales, L. Azpilicueta, and J. A. Galaviz-Aguilar, “Comparative study of channel estimators for massive MIMO 5G NR systems,” *IET Commun.*, vol. 14, no. 7, pp. 1175–1184, Apr. 2020.
- [11] J. Liu, K. Mei, X. Zhang, D. Ma, and J. Wei, “Online extreme learning machine-based channel estimation and equalization for OFDM systems,” *IEEE Commun. Lett.*, vol. 23, no. 7, pp. 1276–1279, Jul. 2019.
- [12] L. Yang, Q. Zhao, and Y. Jing, “Channel equalization and detection with ELM-based regressors for OFDM systems,” *IEEE Commun. Lett.*, vol. 24, no. 1, pp. 86–89, Jan. 2020.
- [13] L. Azpilicueta, P. Lopez-Iturri, J. Zuñiga-Mejia, M. Celaya-Echarri, F. A. Rodríguez-Corbo, C. Vargas-Rosales, E. Aguirre, D. G. Michelson, and F. Falcone, “Fifth-generation (5G) mmwave spatial channel characterization for urban environments’ system analysis,” *Sensors*, vol. 20, no. 18, p. 5360, 2020.
- [14] E. Dahlman, S. Parkvall, and J. Skold, *5G NR: The Next Generation Wireless Access Technology*. New York, NY, USA: Academic, 2018.
- [15] C. Vargas and J. R. Rodríguez, *Wireless Communications*. Monterrey, Mexico: Editorial Digital del Tecnológico de Monterrey, 2010.

- [16] Y. S. Cho, J. Kim, W. Y. Yang, and C. G. Kang, *MIMO-OFDM Wireless Communications With MATLAB*. Hoboken, NJ, USA: Wiley, 2010.
- [17] A. Zaidi, F. Athley, J. Medbo, U. Gustavsson, G. Durisi, and X. Chen, *5G Physical Layer: Principles, Models and Technology Components*. New York, NY, USA: Academic, 2018.
- [18] L. Sanguinetti, E. Björnson, and J. Hoydis, "Toward massive MIMO 2.0: Understanding spatial correlation, interference suppression, and pilot contamination," *IEEE Trans. Commun.*, vol. 68, no. 1, pp. 232–257, Jan. 2020.
- [19] V. Savaux, Y. Louët, M. Djoko-Kouam, and A. Skrzypczak, "Minimum mean-square-error expression of LMMSE channel estimation in SISO OFDM systems," *Electron. Lett.*, vol. 49, no. 18, pp. 1152–1154, 2013.
- [20] M. Celaya-Echarri, L. Azpilicueta, P. Lopez-Iturri, F. Falcone, M. G. Sanchez, and A. Vazquez Alejos, "Validation of 3D simulation tool for radio channel modeling at 60 GHz: A meeting point for empirical and simulation-based models," *Measurement*, vol. 163, Oct. 2020, Art. no. 108038.
- [21] F. A. Rodríguez-Corbo, L. Azpilicueta, M. Celaya-Echarri, P. Lopez-Iturri, I. Picallo, F. Falcone, and A. V. Alejos, "Deterministic 3D ray-launching millimeter wave channel characterization for vehicular communications in urban environments," *Sensors*, vol. 20, no. 18, p. 5284, Sep. 2020.
- [22] C. A. Gutiérrez and M. Cabrera, "Issues of the simulation of wireless channels with exponential-decay power-delay profiles," in *Proc. IEEE 16th Int. Symp. Pers., Indoor Mobile Radio Commun.*, Sep. 2005, pp. 507–511.
- [23] X. Wang, H. Hua, and Y. Xu, "Pilot-assisted channel estimation and signal detection in uplink multi-user MIMO systems with deep learning," *IEEE Access*, vol. 8, pp. 44936–44946, 2020.
- [24] D. F. Carrera, D. Zabala-Blanco, C. Vargas-Rosales, and C. A. Azurdia-Meza, "Extreme learning machine-based receiver for multi-user massive MIMO systems," *IEEE Commun. Lett.*, vol. 25, no. 2, pp. 484–488, Feb. 2021.
- [25] D. Zabala-Blanco, M. Mora, C. A. Azurdia-Meza, and A. D. Firoozabadi, "Extreme learning machines to combat phase noise in RoF-OFDM schemes," *Electronics*, vol. 8, no. 9, p. 921, Aug. 2019.
- [26] M.-B. Li, G.-B. Huang, P. Saratchandran, and N. Sundararajan, "Fully complex extreme learning machine," *Neurocomputing*, vol. 68, pp. 306–314, Oct. 2005.
- [27] C.-L. Xiong, D.-G. Wang, X.-Y. Zhang, J.-B. Wei, and C.-J. Tang, "Recur-sive channel estimation algorithms for iterative receiver in MIMO-OFDM systems," in *Proc. IEEE Wireless Commun. Netw. Conf.*, Apr. 2009, pp. 1–5.



DETERMINISTIC 3D RAY-LAUNCHING MILLIMETER WAVE CHANNEL CHARACTERIZATION FOR VEHICULAR COMMUNICATIONS IN URBAN ENVIRONMENTS.

DIEGO FERNANDO CARRERA (Member, IEEE) received the B.E. degree in electronics and telecommunications engineering from the Private Technical University of Loja, Ecuador, in 2012, and the M.Sc. degree in information technology management and the Ph.D. degree in telecommunications engineering from the Tecnológico de Monterrey, Mexico, in 2015 and 2020, respectively. His research interests include statistical signal processing, channel estimation, symbol



location, interference, network and channel coding, and optimum receiver design. He is currently a member of the Mexican National Researchers System (SNI), the Mexican Academy of Science (AMC), and the Academy of Engineering of Mexico, a Senior Member of the IEEE Communications Society Monterrey Chapter Chair, and the Faculty Advisor of the IEEE-HKN Lambda-Rho Chapter, Tecnológico de Monterrey. He was the Technical Program Chair of the IEEE Wireless Communications and Networking Conference (IEEE WCNC). He is also an Associate Editor of IEEE Access and the *International Journal of Distributed Sensor Networks*.

CESAR VARGAS-ROSALES (Senior Member, IEEE) received the M.Sc. and Ph.D. degrees in electrical engineering from Louisiana State University, with the focus on communications and signal processing. He is the coauthor of the book *Position Location Techniques and Applications* (Elsevier). His research interests include personal communications, 5G/6G, cognitive radio, MIMO systems, stochastic modeling, traffic modeling, intrusion/anomaly detection in networks, position



techniques of artificial intelligence to automate different tasks on new generation networks, such as traffic modeling, intrusion detection systems, and network resources optimization.

NOE M. YUNGAICELA-NAULA received the B.Sc. degree in electronic and telecommunication engineering from the Universidad de Cuenca, Cuenca, Ecuador, in 2015, and the M.Sc. degree in intelligent systems from the Tecnológico de Monterrey, in 2018, where he is currently pursuing the Ph.D. degree. From November 2017 to March 2018, he was a Visiting Scholar with Concordia University, Montreal, QC, Canada. His current research interest includes the use of tech-



Monterrey, Mexico. She has over 150 contributions in relevant journals and conference publications. Her research interests include radio propagation, mobile radio systems, ray tracing, and channel modeling. She was a recipient of the IEEE Antennas and Propagation Society Doctoral Research Award in 2014, the Young Professors and Researchers Santander Universities 2014 Mobility Award, the ECSA 2014 Best Paper Award, the IISA 2015 Best Paper Award, the Best Ph.D. from the Colegio Oficial de Ingenieros de Telecomunicación in 2016, the N² Women Rising Stars in Computer Networking and Communications 2018 Award, and the ISSI 2019 Best Paper Award.

LEYRE AZPILICUETA (Senior Member, IEEE) received the degree in telecommunications engineering, the master's degree in communications, and the Ph.D. degree in telecommunication technologies from the Public University of Navarre (UPNA), Spain, in 2009, 2011, and 2015, respectively. In 2010, she was a Radio Engineer with the Research and Development Department, RFID Osés. She is currently an Associate Professor and a Researcher with the Tecnológico de Monterrey,